IOP Publishing Journal of Physics D: Applied Physics
J. Phys. D: Appl. Phys. **40** (2007) 2285–2292 doi:10.1088/0022-3727/40/8/S07

Factors determining properties of multi-walled carbon nanotubes/fibres deposited by PECVD

M S Bell, K B K Teo and W I Milne

Electrical Engineering Division, Engineering Department, University of Cambridge, 9 J J Thompson Avenue, Cambridge, CB3 0FA, UK

E-mail: kbkt2@cam.ac.uk

Received 18 August 2006, in final form 1 November 2006
Published 4 April 2007
Online at stacks.iop.org/JPhysD/40/2285

Abstract
This paper presents a number of factors which have been found to be important to the growth of carbon nanotubes and nanofibres by plasma enhanced chemical vapour deposition. The effect of the electric field in a plasma discharge on nanotube growth is investigated and shown to be important in achieving nanotube alignment. The use of a plasma discharge also enables deposition to take place at lower temperatures, facilitating the use of substrates which would otherwise be damaged. The effect of varying the ratio of carbon feedstock gas to etchant gas is investigated and the ratio is shown to be important for controlling the shape of deposited nanostructures. The effects of varying plasma power are investigated, showing that greater plasma power results in a lower growth rate. Higher levels of plasma power are also shown to cause the sidewalls of deposited carbon nanotubes to be etched. Finally, the growth rate of carbon nanotubes and nanofibres is shown to depend upon the strength of the local electric field. It is proposed that a higher field causes greater ionization within the plasma, which results in a higher growth rate. This is borne out by comparing simulation results with experimental observations.

1. Introduction

Carbon nanotubes have attracted great interest among researchers since their discovery. Their physical and electronic properties, combined with their chemical inertness, make them potentially useful for applications as diverse as electron-field emitters, nanoelectrodes, filter media and superhydrophobic surfaces.

In this paper, we report on some of the key factors that determine the properties of multi-walled carbon nanotubes and nanofibres deposited by plasma enhanced chemical vapour deposition (PECVD). The definition of a multi-walled carbon nanotube for the purposes of this paper is a structure that consists of concentric graphene cylinders. Less well-ordered structures are referred to as nanofibres. Four key factors that we have found to be important are discussed in the following sections.

2. The presence of plasma during deposition

The most common methods used for the production of carbon nanotubes are arc discharge [1, 2], laser vaporization [3], and chemical vapour deposition (CVD) [4, 5].

When Iijima first reported on the synthesis of carbon nanotubes [6], he used an arc discharge arrangement, similar to an earlier method used by Krätschmer to produce C_{60} [7]. In both arc discharge and laser vaporization, a block of solid graphitic carbon is heated to a very high temperature, resulting in the separation of some carbon atoms from the block. These atoms then reassemble on the cathode in the case of arc discharge and on a cooled collector in the case of laser vaporization. It is during this reassembly that the highly ordered nanotubes are formed.

Catalytic CVD is an entirely different process. Instead of beginning with a block of carbon, carbon atoms are extracted

from a hydrocarbon gas, which dissociates either thermally (thermal CVD) or in the presence of a plasma (PECVD). Once again, the dissociated carbon atoms self-assemble into highly ordered nanotubes; however in this case the nanotubes form on a prepared substrate, which may be made of any suitable medium, for example, silicon or glass. The self-assembly is facilitated by catalyst nanoparticles, which seed the nanotube growth. The size of catalyst particles has been shown to determine the size of the resulting nanotubes [8, 9], as well as to determine their location, so the role of the catalyst is key in device fabrication.

The catalyst takes the form of a transition metal (typically Fe, Ni or Co). It may be applied chemically from a solution containing the catalyst [10] or directly by using techniques such as thermal evaporation, ion beam sputtering [11] or magnetron sputtering [12]. For this work magnetron sputtering was selected, as this provides a well-controlled catalyst thickness of the order of a few nanometres.

There is a further consideration with respect to the catalyst layer. This is the chemical interaction between the catalyst and the substrate at the temperatures encountered during PECVD. If there were to be a reaction, the catalyst material would dissipate, ending its usefulness for seeding nanotube growth. This is, in fact, a problem with using silicon as a substrate with the transition metals listed, as they would all diffuse into the substrate at the temperatures used for carbon nanotube growth (600–700 °C). In order to eliminate this problem, it is necessary to place a diffusion barrier between the silicon substrate and the metal catalyst layer. This diffusion barrier must itself be unaffected by the temperatures encountered during nanotube growth.

SiO_2 is the most obvious material for a diffusion barrier, as it is easily formed on a silicon substrate. If it is desired to make electrical contact with the nanotubes, a conductive diffusion barrier such as TiN [13] or (indium tin oxide) (ITO) can be used.

When heat is applied to the substrate bearing the sputtered film, the increased surface mobility and strong cohesive forces of the catalyst atoms causes the film to coalesce into nanoparticles [14]. The barrier layer is unaffected by the heating. This 'annealing' process is illustrated in figure 1.

The thickness of the catalyst film together with the annealing temperature and duration determines the size of the nanoparticles. There is of course a statistical variation in the observed nanoparticle sizes [15], which ultimately leads to a variation in the diameter of the carbon nanotubes produced.

The ability to deposit carbon nanotubes selectively based upon the location of catalyst particles provides the possibility for lithographic definition of the position of nanotubes and hence for the direct deposition of nanotubes for electronic device applications. It is worth noting that this technique is not new; it was used for many years before the discovery of carbon nanotubes for the deposition of other carbon structures [16]. Thermal CVD requires high temperatures (800–1000 °C) and has two principal disadvantages. Firstly, the high temperature rules out the use of many desirable substrate materials (e.g. glass). Secondly, the carbon nanotubes produced are not just randomly oriented, but they are also curly and spaghetti-like.

PECVD is an alternative technique used extensively in the semiconductor industry, which allows CVD to take place at lower temperatures. The energy in the plasma discharge replaces some of the heat energy, allowing gas dissociation and nanotube formation to take place at lower temperatures (600–700 °C). This lower deposition temperature is very significant, as it allows the use of substrate materials which would be damaged by higher growth temperatures. This is important, for example in the production of carbon nanotube based display devices, which use Corning glass as a substrate for nanotube growth.

PECVD has a further advantage: the electric field aligns the carbon nanotubes during growth [17,18]. This is illustrated in figure 2, which shows nanotubes deposited under similar conditions with and without the presence of plasma.

The alignment of the deposited carbon nanotubes is a key advantage for PECVD over thermal CVD. It allows carbon nanotubes to be deposited with controlled orientation, determined by the direction of the electric field. A number of different techniques are available for creating the plasma. These include rf-PECVD [19], microwave PECVD [20], inductively coupled PECVD [21] and dc glow discharge PECVD [14]. For the work discussed in this paper, dc glow discharge PECVD was chosen. This technique has the advantage of simplicity, as it does not require sophisticated matching networks or high frequency equipment.

3. The ratio of feedstock gas to etchant gas

As discussed, the production of carbon nanotubes may be achieved by the dissociation of carbon atoms from a carbon-rich gas, typically CH_4 or C_2H_2, which then self-assemble in nanotube form on catalyst particles. Whilst this process produces carbon nanotubes, it also produces a large amount of amorphous carbon which is deposited both across the substrate surface and on the walls of the growing nanotube. This amorphous carbon inhibits nanotube formation by covering

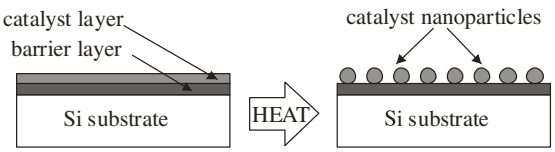

Figure 1. Effect of annealing process on catalyst layer.

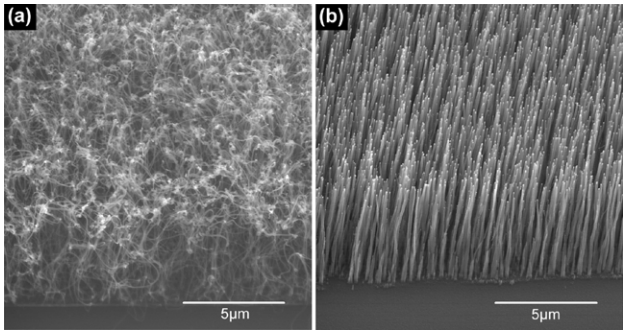

Figure 2. Nanotubes deposited (*a*) without and (*b*) with plasma [9].

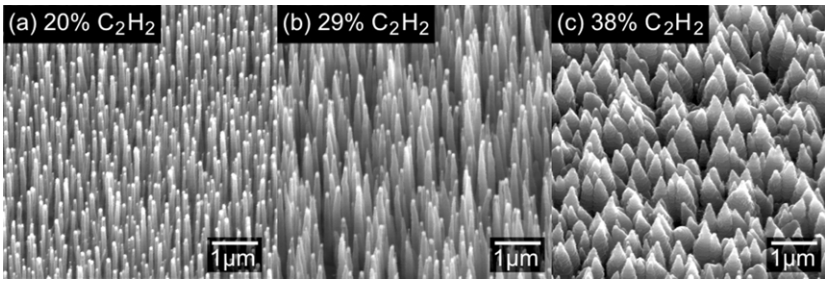

Figure 3. Carbon nanotubes/fibres deposited at different gas ratios [8].

or 'poisoning' the growth catalyst. For a given deposition condition there is a maximum sustainable rate of nanotube self-assembly. If carbon atoms arrive at the catalyst particle at a rate greater than this, the excess carbon precipitates in an amorphous form, which poisons the catalyst.

By combining the carbon feedstock gas with a hydrogen-rich gas, such as H_2 or NH_3, it is possible to reduce or eliminate the production of this amorphous carbon. It is proposed that this is due to the formation of reactive hydrogen species within the plasma which then react with excess carbon atoms, removing them from the site of nanotube nucleation and allowing the self-assembly to continue unhindered.

A detailed parametric study of the growth of carbon nanotubes by PECVD has been previously reported [8]. Of particular interest in this work are the results obtained by varying the ratio of carbon-rich gas (in this case C_2H_2) to hydrogen-rich gas (in this case NH_3).

It was reported that the growth rate for clean, amorphous carbon-free nanotubes peaked at a gas ratio of around 20% C_2H_2 (i.e. 80% NH_3) and that well-aligned carbon nanotubes were grown for C_2H_2 concentrations between 4% and 20%. Above this ratio, the quality diminished significantly with nanofibres being deposited. At 29% C_2H_2 the nanofibres appeared more obelisk-like due to the deposition of excess carbon on the tube sidewalls, and by 38% significant amounts of amorphous carbon were deposited, both on the nanofibre sidewalls and on the substrate. At these higher C_2H_2 concentrations, amorphous carbon was seen to build up on the nanofibre as it grows upwards; as there is more amorphous carbon at the base, the nanofibres appear tip-shaped. These results are shown in figure 3.

In order to understand the mechanisms which lie behind these results, a detailed study of the species present within the plasma during the deposition of carbon nanotubes/fibres was conducted [22]. The plasma during PECVD growth of carbon nanotubes/fibres was investigated using *in situ* measurement. Neutral and positive ion species were extracted from the chamber into a Hiden EQP plasma analyser via a 20 μm diameter aperture which was immersed in the plasma. Mass spectrometry was then performed on the extracted species.

In order to investigate why optimal growth occurs at around 20% C_2H_2 and the processes underlying the production of different forms of carbon at different gas ratios, a series of mass spectrum measurements was taken whilst the volume flow rate proportion of C_2H_2 in the $NH_3 : C_2H_2$ plasma was varied between 0% and 70%. All other parameters were maintained at their standard setting.

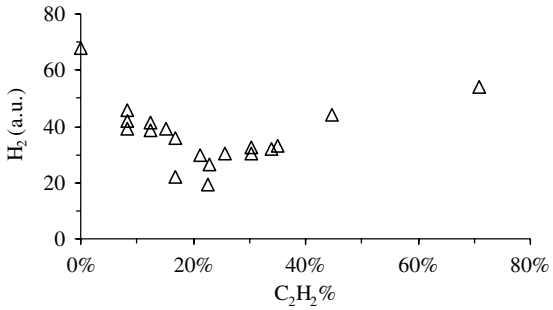

Figure 4. Variation of H_2 data with gas ratio.

The major neutral species detected, aside from NH_3 and C_2H_2, were H_2, N_2 and HCN. This is consistent with data reported by other authors [23]. The dominant ion species detected were NH_3^+ and $C_2H_2^+$.

The results for H_2 are shown in figure 4.

To the left of the figure, where the plasma is predominantly NH_3, it can be seen that the amount of H_2 generated increases as the proportion of NH_3 in the plasma increases, indicating that in this region the H_2 is derived from decomposition of NH_3. To the right of figure 4, where the plasma is predominantly C_2H_2, it can be seen that the amount of H_2 generated rises as the proportion of C_2H_2 rises. In this region, therefore, H_2 is derived from the decomposition of C_2H_2.

At high NH_3 ratios, NH_3 decomposes preferentially over C_2H_2 due to the relative weakness of its molecular bonds. This allows the C_2H_2 to decompose slowly, generating the controlled amounts of carbon necessary for nanotube formation and giving rise to clean, well-aligned carbon nanotubes. At high C_2H_2 ratios, there is insufficient NH_3 to effectively suppress C_2H_2 decomposition, resulting in higher levels of carbon generation and the deposition of amorphous carbon onto the substrate, as observed in figure 3(*b*) and (*c*). NH_3 therefore has two key roles in the formation of carbon nanotubes: not only does it generate atomic hydrogen species which remove excess carbon but it also suppresses the decomposition of C_2H_2, limiting the amount of carbon generated at source.

Chhowalla showed that the growth rate of clean carbon nanotubes in an $NH_3 : C_2H_2$ plasma is at a maximum at around 20% C_2H_2 [8]. This is close to the observed minimum in H_2 at around 23% C_2H_2. It is suggested that a gas ratio of 20–21% C_2H_2 is the optimum condition for nanotube growth. This is close to the minimum in H_2 but with a small margin to ensure that amorphous carbon is not deposited. At this

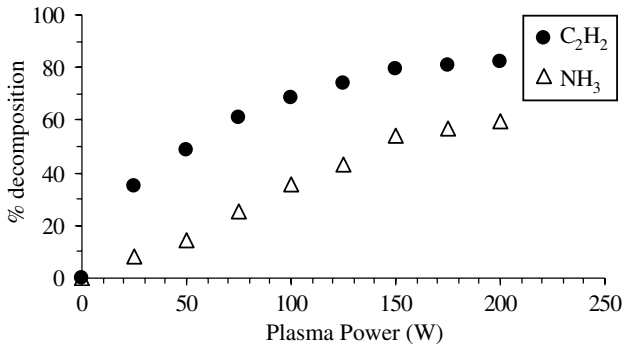

Figure 5. Variation of decomposition of NH_3 and C_2H_2 with plasma power.

point, species which remove carbon are at a minimum and C_2H_2 decomposition is low, giving rise to steady, controlled deposition of carbon nanotubes.

There has been some discussion in the literature regarding the nature of the carbon precursor for the formation of carbon nanotubes. In the recorded mass spectra, C_2, CH_4 or other higher carbon species were not detected and it was thus concluded that, in this case, C_2H_2 is the dominant precursor for nanotube formation. Other authors [24] have detected the presence of C_2H_2 in a $CH_4 : H_2 : NH_3$ plasma yielding carbon nanotubes, which suggests that C_2H_2 may have a key role in nanotube growth. It is also worth noting that C_2H_2 was reported to be the most efficient carbon feedstock for the growth of carbon filaments long before the discovery of carbon nanotubes [25].

4. The level of plasma power

During the deposition of carbon nanotubes discussed so far, the substrate was in all cases heated by tungsten filaments embedded within the graphite stage. However, the plasma power of approximately 60 W provided additional heating above and beyond that generated by the tungsten filaments. In order to investigate the effects of varying the plasma power, a series of measurements were made with substrate heating being provided by plasma power alone. To generate a sufficiently high plasma power, these experiments were conducted at a pressure of 12 mbar.

A series of mass spectrum measurements for neutral species was made at plasma powers ranging from 25 to 200 W. For these experiments, the gas flow rates were fixed at 200 sccm NH_3 and 54 sccm C_2H_2 to give a gas ratio of 21% C_2H_2, the optimum ratio determined in the experiments described above.

The decomposition of NH_3 and C_2H_2 at different levels of plasma power may be measured by comparing the mass spectrum data for NH_3 and C_2H_2 with the corresponding data at room temperature and in the absence of any plasma. The results of this analysis are shown in figure 5.

Figure 5 shows an increase in gas decomposition with increasing plasma power. Having observed this, an exercise was undertaken to compare carbon nanotubes grown under the same conditions of gas flow, temperature and pressure, but with heating being provided by a combination of tungsten heaters and plasma in one case and purely by plasma heating in the other [26].

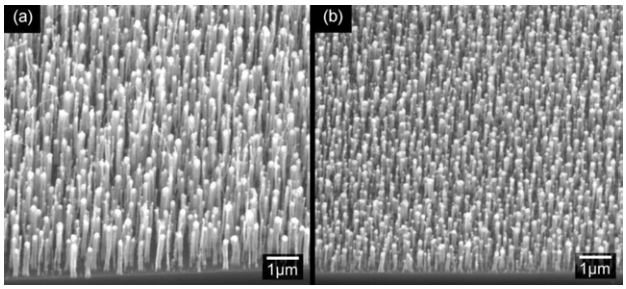

Figure 6. Nanotubes deposited (*a*) using resistive and plasma heating, and (*b*) using purely plasma heating [26].

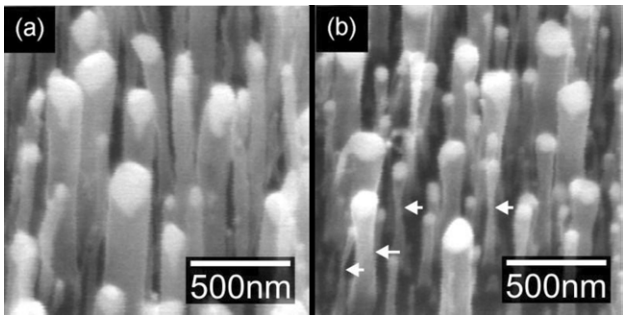

Figure 7. Detail of nanotubes deposited (*a*) using resistive and plasma heating, and (*b*) using purely plasma heating [26].

Two depositions, each of 15 min duration, were undertaken using Si substrates coated with a 15 nm thick barrier layer of ITO and a 7 nm thick layer of Ni catalyst. The first deposition took place using a combination of resistive heating and 66 W plasma power, and the second deposition took place using no resistive heating and 200 W of plasma power. All other conditions were identical, with chamber pressure maintained at 12 mbar and deposition temperature maintained at 700 °C. The results of the two depositions are shown in figure 6.

Figure 6 shows that, under otherwise identical conditions, the growth rate for the nanotubes with purely plasma heating is considerably lower than that for combined resistive and plasma heating. In order to understand why this might be the case, recall that it was determined earlier that C_2H_2 is the dominant precursor for the growth of carbon nanotubes in this system.

Figure 5 shows how the level of C_2H_2 decomposition varies with plasma power. For the nanotubes grown with combined resistive and plasma heating, the plasma power was 66 W, corresponding to approximately 55% C_2H_2 decomposition. For the nanotubes grown with purely plasma heating, the plasma power was 200 W, corresponding to 82% C_2H_2 decomposition. There is much less C_2H_2 available for nanotube growth in the purely plasma heating case compared with the case of combined resistive and plasma heating. A lower growth rate should therefore be expected for the purely plasma heating case, as clearly demonstrated in figure 6.

Looking at the nanotube samples in more detail, another difference is apparent. Figure 7 shows the same images at a higher level of magnification.

Figure 7 shows that in the case of purely plasma heating, the nanotubes are slightly etched, as highlighted by the arrows which show where undercutting has taken place. Again, the

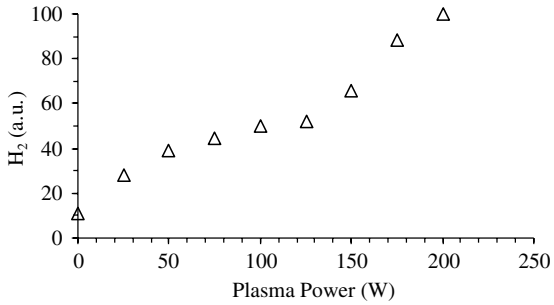

Figure 8. Variation of H_2 signal with plasma power.

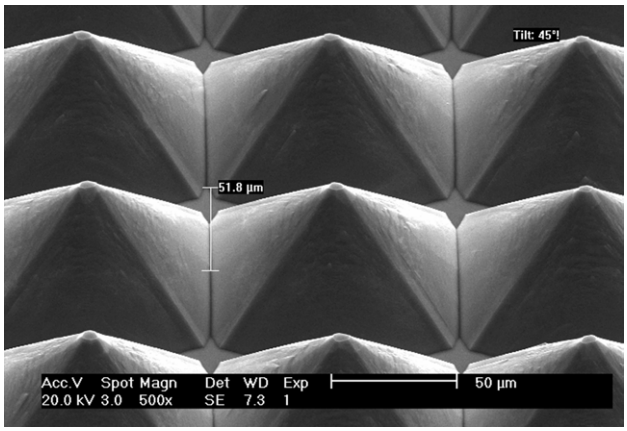

Figure 9. Shaped silicon substrate.

mass spectrometer data provides an insight. It was shown earlier that atomic hydrogen was responsible for removal of excess carbon during nanotube deposition. The data for H_2 for varying plasma power is shown in figure 8.

Figure 8 shows that the amount of H_2 present in the plasma increases with increasing plasma power. This is a consequence of the greater levels of decomposition of C_2H_2 and NH_3. This increased level of hydrogen in the plasma etches carbon and explains the observed undercutting of the nanotube structures at high levels of plasma power.

5. The strength of the electric field

Finally, an investigation was undertaken in order to determine what effect, if any, the strength of the electric field in the plasma may have on the growth of carbon nanotubes/fibres. Varying this field strength without changing any other parameters is difficult, as increasing the voltage in a dc plasma also increases the plasma power, which we have shown causes a significant reduction in the nanotube growth rate due to the increased dissociation of the feedstock gas.

It is, of course, only necessary to vary the electric field strength close to the substrate, where nanotube/fibre growth takes place. By shaping the substrate, it is possible to generate local geometric field enhancement. This allows a higher local electric field to be achieved without varying any other parameters.

A shaped silicon substrate was produced by wet chemical etching, as shown in figure 9.

In order to deposit nanofibres only on the tips of the pyramids on the shaped substrate, catalyst material was selectively deposited on the tips. This could have been achieved using electron beam lithography, but a simpler solution was achieved by spin coating the shaped substrate with a thick layer of PMMA resist to a height just below that of the pyramids, leaving only the tips exposed. ITO barrier and nickel catalyst layers were then sputtered as before, to thicknesses of 15 nm and 7 nm, respectively. The PMMA resist was dissolved in solvent, leaving the barrier and catalyst material on the pyramid tips as required. Carbon nanofibres were deposited simultaneously on both flat and shaped silicon substrates in a PECVD process using NH_3 and C_2H_2 as before.

It was found that the nanofibres deposited on the tips of the shaped substrate were significantly longer than those grown on a flat substrate. This was shown to be true for both 'forests' of nanofibres and individual nanofibres, as illustrated in figures 10 and 11.

Figure 10 shows that the nanofibres in the forest grown on the pyramid tip are approximately two and a half times the length of the nanotubes in the forest grown on flat substrate. Figure 11 shows that the individual nanofibres on the pyramid tips are approximately twice as long as those grown on a flat substrate. Note that the growth times were different for the 'forests' and the isolated nanofibres.

Given that in each case the longer and shorter nanotubes/nanofibres were deposited simultaneously, on substrates which had undergone identical processing (with the exception of chemical etching), many potential reasons for the difference were ruled out. There was no difference in the pre-deposition steps such as wafer cleaning and sputtering of catalyst and barrier layers as these were done together. There was no difference in the temperature, pressure, duration or location of the substrates during nanotube/nanofibre growth. In short, the processing steps followed were identical in each case, with the only difference being the shape of the silicon substrate.

By a process of elimination, the only difference between the depositions which took place on pyramid tips and the depositions which took place on flat areas of the substrate is in the local electric field strength at the deposition site. The electric field is greater around the pyramid tips due to the geometric field enhancement caused by the shaped substrate.

There has been limited study of the effect of electric field strength on the growth rate of carbon nanotubes in published literature. Chhowalla [8] measured the effect of bias voltage on nanotubes deposited in a similar dc-PECVD arrangement, reporting that an increase in bias voltage resulted in a decrease in the rate of nanotube growth. However, increasing the bias voltage also increases plasma power. As was shown earlier, increased plasma power results in increased C_2H_2 decomposition, and so a lower growth rate would be expected.

To investigate the electric field around the carbon nanotubes/nanofibres during deposition, it is necessary to consider the profile of the electric field in dc glow discharge plasma, such as that used to deposit the nanotubes and nanofibres. In dc glow discharge plasma, the voltage between the anode (the gas showerhead in this work) and cathode (the substrate stage in this work) varies as shown in figure 12.

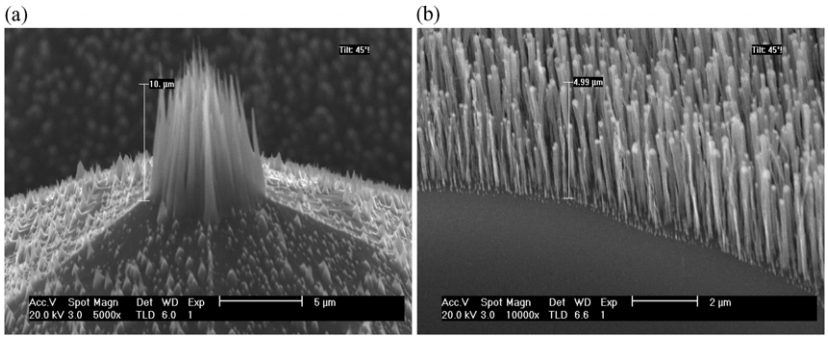

Figure 10. Carbon nanotube/nanofibre 'forests' grown on pyramid (*a*) tip and (*b*) flat substrate.

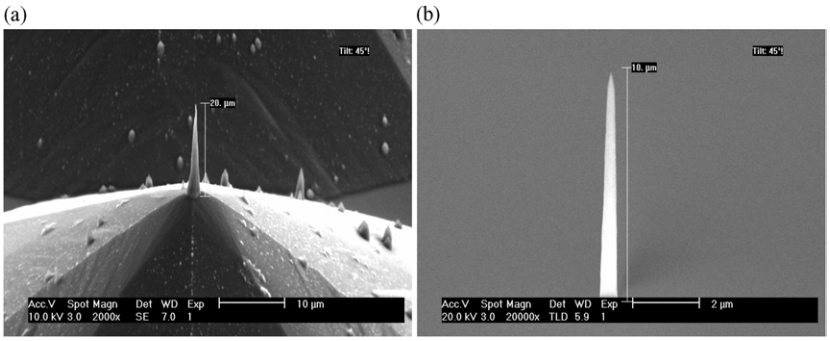

Figure 11. Individual carbon nanofibres grown on pyramid (*a*) tip and (*b*) flat substrate.

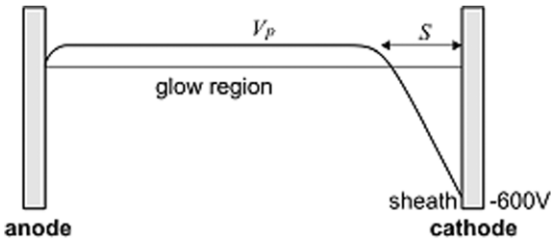

Figure 12. Voltage variation in a dc glow discharge plasma [27].

The plasma has potential V_p in the glow region. A sheath, extending a distance S, is formed close to the cathode, which is also the substrate stage in our experiments. It has been shown [27] that the extent of the high field sheath region in the glow discharge arrangement used in this work is approximately 2 mm, easily sufficient to encompass both the substrate and the growing nanotubes/nanofibres. The nanotubes/nanofibres, which are negatively biased at the cathode, experience a force opposite to the direction of the field (i.e. towards the anode) at their tip which guides them vertically during growth.

Having ascertained that the nanotubes/nanofibres are contained within the high field sheath region during growth, a more detailed investigation of the field around the substrate was undertaken. A three-dimensional electrostatic model of a shaped substrate produced using the finite element package *Gmsh* [28] was used to investigate the shape of the field. Both a flat substrate and a shaped substrate were modelled, in order to allow comparisons to be made.

In each case, the counter electrode was set to be 2 mm above the substrate in order to simulate the effect of the electric field within the plasma sheath. The silicon pyramids in the

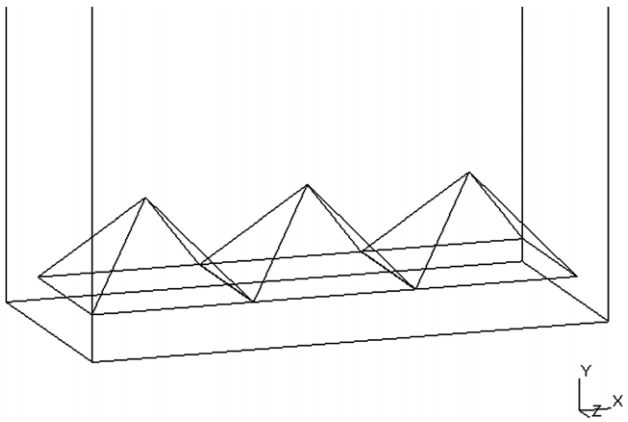

Figure 13. Three-dimensional model of shaped substrate.

shaped substrate case were constructed with a face angle of 48° from the vertical, consistent with measurements made of the actual substrates used. The substrate end of the model for the shaped substrate case is shown in figure 13.

A voltage was applied between the substrate and counter electrode, and finite element analysis used to calculate the potential at points throughout the three-dimensional space. A slice through the vertices of the pyramids showing lines of equipotential is shown in figure 14.

In the flat substrate case, the electric field between the substrate and counter electrode is uniform. In the case of the shaped substrate, the field enhancement of the pyramids causes the field to be higher close to the pyramid tips, though it falls rapidly with vertical distance. The calculated field strength for varying distance above a pyramid tip is shown in figure 15.

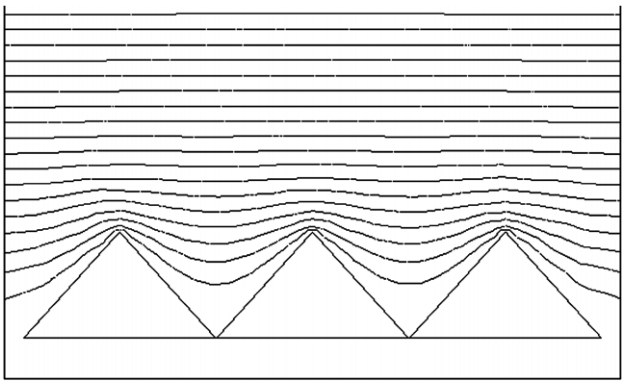

Figure 14. Simulated equipotentials around pyramid tips.

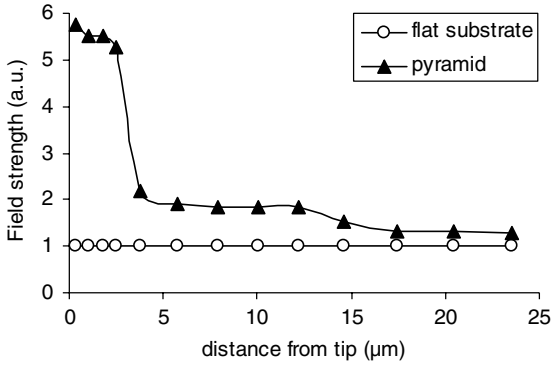

Figure 15. Field strength above pyramid tip.

Figure 15 shows that the field strength immediately above a pyramid tip is between five and six times greater than the uniform field seen with a flat substrate, and that whilst it falls rapidly with distance, at a distance of 20 μm above the pyramid tip it is still higher than the field in the flat substrate case.

Having established how the field strength varies with distance from the pyramid tip, it was necessary to relate this to the rate of nanofibre growth. The nanofibres deposited in this work follow a 'tip growth' model due to the weak interaction between the catalyst material and the barrier layer. As such, the field strength determining growth rate might logically be expected to be that close to the tip of the growing nanofibre.

By assuming that the growth rate at any point is proportional to the local field strength at the top of the growing nanofibre, and by initially neglecting any effect the nanofibre itself may have on the local field strength, it was possible to calculate how the length of nanofibres deposited upon flat and shaped substrates should evolve with time. The results of this calculation are shown in figure 16.

From figure 16, a 10 μm nanofibre grown on a pyramid should correspond to a 4.2 μm nanotube grown on a flat substrate. This is in very good agreement with the nanotube and nanofibre lengths shown in figure 10. Also, a 10 μm nanofibre grown on a flat substrate should correspond to a 19 μm nanofibre grown on a pyramid. Again, this is in very good agreement with the nanofibre lengths shown in figure 11.

The agreement of these calculations with experimental observation is extremely good; however before forming a definitive view, it is worth considering the alternative scenarios.

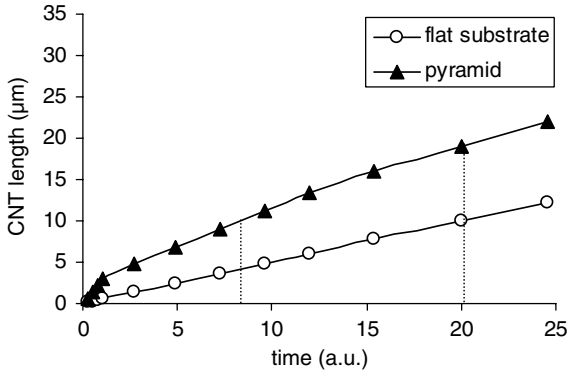

Figure 16. Calculated evolution of nanofibre length.

If the growth rate depended upon the field at the base of the growing nanofibre rather than the field at its tip, figure 15 shows that nanofibres grown on pyramid tips would be expected to be five to six times longer than in the flat substrate case for all deposition times. This 'base growth' model is not consistent with experimental observations.

Alternatively, if the additional field enhancement caused by the growing nanofibre affected the growth rate, the lengths of nanofibres grown on flat areas of substrate and on pyramids would diverge exponentially, giving differences far in excess of those observed by experiment.

Since neither of the alternatives fit with experimental data, and as the fit to the first model is good, it is proposed that the nanofibre growth rate is proportional to the local electric field close to the nanofibre tip, neglecting any effect the growing nanofibre may have on this.

In order to understand why this may be the case, it is necessary to consider what part the electric field in the plasma plays in the growth of carbon nanotubes and nanofibres. It was shown earlier that simply increasing the plasma power resulted in a lower growth rate, as there was greater dissociation of C_2H_2, the precursor for nanotube and nanofibre growth.

However, an increase in the local electric field within the glow discharge plasma by geometric enhancement leads to an increased level of gas ionization within a localized area without an overall increase in the level of dissociation of C_2H_2. It is proposed that the higher local electric field close to the tips of the silicon pyramids leads to a greater abundance of $C_2H_2^+$ ions in that region and that it is these ions which provide the carbon feedstock for the growth of carbon nanotubes and nanofibres on the negatively biased substrate.

Increasing the degree of ionization within the plasma does not change the balance between species which encourage the deposition of carbon ($C_2H_2^+$) and species which remove excess carbon (H^+). Rather it results in greater density of both $C_2H_2^+$ and H^+ species. This in turn leads to a balance, as previously, between the rate of carbon deposition and the rate of carbon abstraction, resulting in steady nanofibre growth. However, as both of these rates are higher than before, the result is a higher net carbon deposition rate and hence a higher rate of nanofibre growth.

This explains why the growth rate is higher, but does not explain why it is affected by the shape of the substrate but not by the shape of the growing nanofibres. In order to understand this, it is necessary to consider the extent of the higher field

region. The volume within which the field is significantly influenced by the nanofibres is small when compared with the volume affected by the shape of the substrate. The number of ions generated is therefore not significantly affected by this localized higher field, whereas it is affected by the field enhancement caused by the shaping of the substrate. This is in line with experimental observations.

6. Summary

It has been shown that the electric field present in a plasma discharge aligns nanotubes and nanofibres during CVD, allowing structures to be created which are much more suitable for electronic applications than structures deposited using thermal CVD. It has further been shown that the use of a plasma discharge enables nanotube and nanofibre deposition to take place at lower temperatures, facilitating the use of substrates which would not survive the higher temperatures necessary for thermal CVD.

The importance of the ratio of carbon feedstock gas to etchant gas for depositing high quality nanotubes and nanofibres has been demonstrated. The process by which nanotubes and nanofibres are deposited requires a careful balance between carbon deposition and carbon removal reactions in order to generate high quality nanostructures.

The effects of varying plasma power have been investigated. It has been shown that greater plasma power results in greater dissociation of the carbon feedstock gas, leading to a lower supply of C_2H_2, the key precursor for nanotube growth in these experiments. This in turn results in a lower growth rate. The effect of the higher dissociation has also been observed in an increased generation of active hydrogen species which etch the sidewalls of the deposited carbon nanotubes.

Finally, it has been demonstrated experimentally that the growth rate of carbon nanotubes and nanofibres depends critically upon the strength of the electric field in the region in which deposition takes place. It is proposed that a higher field results in a higher level of ionization within the plasma, which in turn results in a higher growth rate.

Acknowledgments

MSB acknowledges discussions with Professor John Robertson. This work was funded by the Engineering and Physical Sciences Research Council. KBKT acknowledges the support of the Royal Academy of Engineering and Christ's College, Cambridge.

References

[1] Ebbesen T W and Ajayan P M 1992 *Nature* **358** 220
[2] Journet C, Maser W K, Bernier P, Loiseau A, delaChapelle M L, Lefrant S, Deniard P, Lee R and Fischer J E 1997 *Nature* **388** 756
[3] Thess A *et al* 1996 *Science* **273** 483
[4] Fan S, Chapline M G, Franklin N R, Tombler T W, Cassell A M and Dai H 1999 *Science* **283** 512
[5] Ren Z F, Huang Z P, Xu J W, Wang J H, Bush P, Siegal M P and Provencio J H 1998 *Science* **282** 1105
[6] Iijima S 1991 *Nature* **354** 56
[7] Krätschmer W, Lamb L D, Fostiropolous K and Huffman D R 1990 *Nature* **347** 354
[8] Chhowalla M, Teo K B K, Ducati C, Rupesinghe N L, Amaratunga G A J, Ferrari A C, Roy D, Robertson J and Milne W I 2004 *J. Appl. Phys.* **90** 5308
[9] Choi Y C, Shin Y M, Lim S C, Bae D J, Lee Y H, Lee B S and Chung D 2000 *J. Appl. Phys.* **88** 4898
[10] Cassell A M, Verma S, Delzeit L, Meyyappan M and Han J 2001 *Langmuir* **17** 260
[11] Delzeit L, Nguyen C V, Stevens R M, Han J and Meyyappan M 2002 *Nanotechnology* **13** 280
[12] Choi Y C, Lee Y H, Lee B S, Park G, Choi W B, Lee S and Kim J M 2000 *J. Vac. Sci. Technol.* A **18**, 1864
[13] Rao A M, Jacques D, Haddon R C, Zhu W, Bower C and Jin S 2002 *Appl. Phys. Lett.* **76** 3813
[14] Merkulov V I, Lowndes D H, Wei Y Y, Eres G and Voelkl E 2002 *Appl. Phys. Lett.* **76** 3555
[15] Bower C, Zhou O, Zhu W, Werder D J and Jin S H 2000 *Appl. Phys. Lett.* **77** 2767
[16] Baker R T K, Barber M A, Harris P S, Feates F S and Waite R J 1972 *J. Catal.* **26** 51
[17] Teo K B K, Chhowalla M, Amaratunga G A J, Milne W I, Pirio G, Legagneux P, Wyczisk F, Olivier J and Pribat D 2002 *J. Vac. Sci. Technol.* B **20** 116
[18] Delzeit L, McAninch I, Cruden B A, Hash D, Chen B, Han J and Meyyappan M 2002 *J. Appl. Phys.* **91** 6027
[19] Boskovic B O, Stolojan V, Khan R U A, Haq S and Silva S R P 2002 *Nature Mater.* **1** 165
[20] Bower C, Zhu W, Jin S and Zhou O 2000 *Appl. Phys. Lett.* **77** 830
[21] Li J, Stevens R, Delzeit L, Ng H T, Cassell A, Han J and Meyyappan M 2002 *Appl. Phys. Lett.* **81** 910
[22] Bell M S, Lacerda R G, Teo K B K, Rupesinghe N L, Chhowalla M, Amaratunga G A J and Milne W I 2004 *Appl. Phys. Lett.* **85** 1137
[23] Cruden B A, Cassell A M, Ye Q and Meyyappan M 2003 *J. Appl. Phys.* **94** 4070
[24] Woo Y S, Jeon D K, Han I T, Lee N S, Jung J E and Kim J M 2002 *Diamond Relat. Mater.* **11** 59
[25] Baker R T K and Harris P S 1978 *Chem. Phys. Carbon* **14** 83
[26] Teo K B K *et al* 2004 *Nano Lett.* **4** 921
[27] Bell M S, Teo K B K, Lacerda R G, Milne W I, Hash D B and Meyyappan M 2006 *Pure Appl. Chem.* **78** 1117
[28] Geuzaine C and Remacle J-F 2006 Gmsh: a three-dimensional finite element mesh generator with built-in pre- and post-processing facilities, http://www.geuz.org/gmsh/